

- ⁷W. F. Egelhoff, J. W. Linnett, and D. L. Perry, Phys. Rev. Lett. **36**, 98 (1976).
- ⁸B. Feuerbacher and R. F. Willis, Phys. Rev. Lett. **37**, 446 (1976).
- ⁹C. Noguera, D. Spanjaard, D. Jepsen, Y. Ballu, C. Guillot, J. Lecante, J. Paigne, Y. Pétrouff, R. Pinchaut, and R. Cini, Phys. Rev. Lett. **38**, 1171 (1977).
- ¹⁰S.-L. Weng, T. Gustafsson, and E. W. Plummer, Phys. Rev. Lett. **39**, 822 (1977).
- ¹¹C. P. Kerker, A. Zunger, K. M. Ho, and M. L. Cohen, Bull. Am. Phys. Soc. **23**, 364 (1978).
- ¹²J. E. Inglesfield, Surf. Sci. **76**, 379 (1978), and to be published.
- ¹³E. W. Plummer and A. E. Bell, J. Vac. Sci. Technol. **9**, 583 (1972).
- ¹⁴T. V. Vorburger, D. Penn, and E. W. Plummer, Surf. Sci. **48**, 417 (1975), and references therein.
- ¹⁵M. W. Holmes and D. A. King, to be published.
- ¹⁶J. E. Inglesfield, Surf. Sci. **76**, 355 (1978).
- ¹⁷Results showing the agreement between the dispersion of the surface state and that of the center of gravity of the absolute band gap between the third and fourth bands, as projected into the {110} SBZ, will be presented in Ref. 15.
- ¹⁸G. V. Hansson and S. A. Flodström, Phys. Rev. B **18**, 1562 (1978).
- ¹⁹P. Soven, E. W. Plummer, and N. Kar, Crit. Rev. Solid State Sci. **6**, 111 (1976).

Chemically Induced Charge Redistribution at Al-GaAs Interfaces

L. J. Brillson

Xerox Webster Research Center, Webster, New York 14580

and

R. Z. Bachrach, R. S. Bauer, and J. McMenamin

Xerox Palo Alto Research Center, Palo Alto, California 94304

(Received 6 October 1978)

We show that the exchange reaction between Al and GaAs at the microscopic interface produces a charge redistribution in two stages which determines Schottky-barrier formation.

The nature of charge distribution at microscopic metal-semiconductor (M-S) interfaces has attracted considerable attention in recent years because of its relation to Schottky barrier (S-B) formation. Barrier heights of junctions exhibiting a wide range of interface behavior¹ have been related to dipole layers resulting from changes in these local charge distributions.^{2,3} Local charge densities have been used in self-consistent pseudopotential calculations to account for the electronic structure and S-B height of a variety of M-S interfaces.^{4,5} These calculations assumed a jellium core potential for the metal side of the interface which does not adequately describe the detailed atomic bonding at the interface of the local electronic structure observed for metals such as Al.⁶ Because interface chemical reactions greatly modify the phases at M-S junctions^{3,7-12} and thereby play a central role in S-B formation, realistic calculations of M-S electronic properties are possible only if the interface atomic microstructures are known. In this Letter, we report the first microscopic electronic and chemical characterization of a relatively abrupt, compound semiconductor interface—Al

on GaAs(110). Metal-induced surface-state phenomena have already been reported for In¹³ and Au¹¹ on GaAs(110). Here we provide a more complete picture of the changes in chemical bond configuration which redistribute charge near the interface and demonstrate that the resultant dipole determines the S-B height of the macroscopic junction. The chemical-structure and charge-redistribution measurements thus provide key parameters for initiating (and evaluating) calculations of interface electronic structure.

The Al-GaAs interface formed by evaporating increasing film thicknesses of Al onto cleaved GaAs(110) surfaces at room temperature in ultra-high vacuum was studied by an assortment of techniques. Chemical structure was determined using Auger-electron spectroscopy (AES), low-energy-electron diffraction (LEED), and synchrotron-radiation-excited photoemission. Surface-work-function ϕ_s , band-bending qV_B , and surface-photovoltage-spectroscopy (SPS) measurements were performed with a vibrating Kelvin probe. Contact-potential measurements were carried out in the absence of electron beams which could affect the results substantially.

Core-level and plasmon excitations were monitored by low-energy-electron-loss spectroscopy (ELS). Synchrotron measurements were carried out on the 4° beam line of the Stanford Synchrotron Radiation Laboratory. Al deposition was monitored by a quartz-crystal oscillator during evaporation. Each experiment was carried out in <12 h to minimize C and O contamination, which AES showed to be negligible.

Both AES and core-level photoemission allowed chemical effects to be followed as the interface was formed. Both gave a consistent picture which is summarized below. Analysis of the Al 2*p*, As 3*d*, and Ga 3*d* core-level signals at the shortest escape depths available shows a monotonic decrease of both Ga and As with increasing Al coverage. Above 5-Å Al coverage, the Ga and As signals do not fall off exponentially, indicating diffusion. Over 200 Å of Al are required before As is no longer observed with 130-eV excitation. AES analysis of the Al, Ga, and As LMM peaks indicates the same Ga and As diffusion in Al. Ga and As diffusion also occurs for Au on GaAs.¹¹

Figure 1 shows core-level photoemission spectra as a function of Al coverage. Chemical shifts as well as intensity changes are observed for both the Al 2*p* and Ga 3*d* levels. The As 3*d* (not shown) decreases in intensity with only a ~0.1-eV shift to higher binding energy after taking the Fermi-level shift into account. Also not shown are valence-band spectra which exhibit a sharp decrease in the As-derived features with initial overlayer coverages, further indicating that Al islands do not form.¹⁰ By deconvoluting the Al

spectra, one obtains a chemical shift of 0.7 eV to higher binding energy. Similar deconvolution of the Ga spectra yields a 0.95-eV shift to lower binding energy, compared to the 1.1-eV shift of free Ga relative to GaAs.¹⁴ The very small As shift and the formation of nearly free Ga indicates that As is reacted as AlAs. The relative areas of the deconvoluted Ga and Al peaks can be used as a measure of interfacial composition. Taking the relative Al/Ga areas of 0.20 with an empirical escape depth of 6.5 Å, one finds that the outermost layer is completely exchanged for Al coverages up to a monolayer. Also, the Al KLL AES structure exhibits a single chemically shifted value of 63 eV vs 68 eV for the bulk overlayer, indicating that all of the deposited atoms react with the GaAs substrate. Furthermore, 100-eV ELS measurements exhibit spectral features corresponding to interband transitions at 3.0 and 5.7 eV for the initial Al overlayers which are shifted to lower energy relative to the analogous GaAs features at 3.8 and 6.7 eV.⁹ The shifted features are characteristic of AlAs epitaxial layers measured under similar conditions.¹⁵ Spectra obtained with low incident-beam intensity (<1 μA/cm²) and rapid signal averaging displayed no time-dependent electron-beam effects. Thus the interfacial layer is completely AlAs, and the reaction drives out subsurface Ga. Some Ga continues to segregate to the surface of the Al with increasing thickness so that the metallic-alloy side of the interface changes with increasing Al thickness. The Ga 3*d* chemical shift increases to 1.1 eV for thicker films, indicating finite Ga bond strength across the interface for the initial exchange reaction.

The LEED pattern of Al on GaAs(110) remains characteristic of an ordered surface for metal coverages up to ½ monolayer. However, while the spot pattern is essentially unchanged, the LEED intensity profiles of the (10), (1̄1), (11), and (01̄) diffracted beams are substantially altered by the Al and reflection symmetry is removed between the (1̄0) and (10), (1̄1̄) and (11̄), and (1̄1) and (11) beams. These changes are consistent with the exchange reaction and a lower surface symmetry due to the segregated Ga. Deposition of additional Al removes the ordered LEED pattern in this case as a disordered Al overlayer formed.

The shift in bond strength away from the surface Ga and into the Al-As bonds produces a charge redistribution which can be measured from the interface dipole formed. The dipole voltage Δχ can be expressed as Δχ = Δφ_s - ΔqV_B,

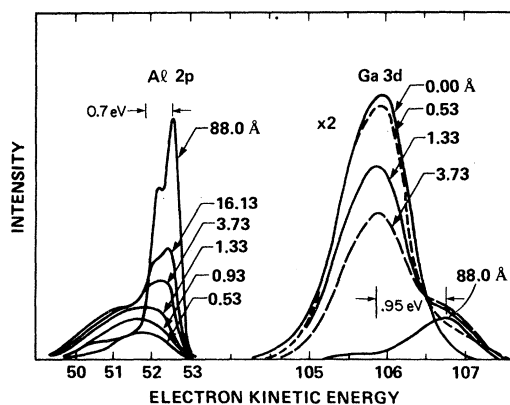


FIG. 1. Core-level photoemission spectra (130-eV excitation) of chemically shifted Al 2*p* and Ga 3*d* core-level spectra for various Al overlayer thicknesses.

where ϕ_s is the surface work function and qV_B is the band bending within the surface-space-charge region of GaAs. These are shown schematically in the Fig. 2 inset. qV_B is determined from the flattening of the bands under intense ($>10^{18}$ photons/cm²) bandgap illumination from a 150-W Xe lamp. The Fermi-level position with respect to the band edges also follows from ϕ_s and qV_B . Figure 2 illustrates how ϕ_s and qV_B vary from their cleaved GaAs(110) surface values with increasing Al coverage. As shown, ϕ_s increases with submonolayer coverage, reaching a maximum at 4.0×10^{14} atoms/cm² (0.7 Å). With further coverage, ϕ_s decreases monotonically, reflecting the change in the metallic-alloy composition. In contrast, qV_B increases by 0.44 eV from an initial value of 0.02 eV, but does not saturate at monolayer coverage. The visually smooth, mirrorlike cleavage surfaces exhibited a low initial band-bending value, consistent with a low cleavage-step density.¹⁶ SPS measurements reveal no evidence for any intrinsic surface states within the band gap for this surface. The difference $\Delta\phi_s - \Delta qV_B$ at 0.7-Å Al coverage yields a negative dipole (i.e., surface more negative than layers below) with $\Delta\chi = 0.24 \pm 0.09$ eV. The dipole moment follows from the ϕ -versus-thickness derivative at zero thickness¹⁷ and equals 0.34 ± 0.13 electrons Å/atom. The maximum dipole voltage occurs at 0.7 Å, i.e., half monolayer. Thus, we conclude that the dipole formation is directly related to the reaction of Al with As at Ga surface sites.

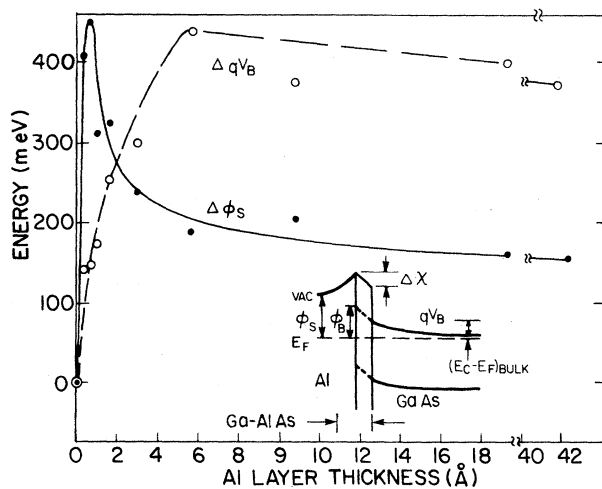


FIG. 2. Variation of surface work function ϕ_s and GaAs band bending qV_B vs Al overlayer thickness. Inset illustrates interface dipole $\Delta\chi$ schematically.

The dipole voltage also determines the S-B height of the Al-GaAs interface. The Fig. 1 inset shows the barrier height $\phi_B = qV_B + (E_c - E_F)_{\text{bulk}} + \Delta\chi$, where qV_B is the band bending after Al deposition and $(E_c - E_F)_{\text{bulk}} = 0.01$ eV as determined by the bulk doping ($n = 3.2 \times 10^{17}$ Te). For $\Delta\chi = 0.24$ eV in Fig. 3, the S-B height $\phi_B = 0.71 \pm 0.08$ eV. Literature values for Al-GaAs S-B heights measured by internal photoemission and capacitance methods are typically 0.8 eV.¹⁸ Cho and Dernier have recently measured interface barrier heights formed by molecular-beam epitaxy of 0.66 eV for As-stabilized GaAs(100) and 0.72 eV for Ga-stabilized GaAs(100).¹⁹

The slow decrease of ϕ_s for thicknesses above the initial dipole formation reflects the formation of bulk Al only after several metal monolayers as well as the continued diffusion of Ga and As into the overlayer. The face-dependent work function of Al ranges between $\phi_{\text{Al}} = 4.25\text{--}4.35$ eV,²⁰ compared with $\chi_{\text{GaAs}} + (E_c - E_F)_{\text{bulk}} = 4.1$ eV in bulk GaAs. Clearly, simple charge transfer out of the GaAs surface-space-charge region into the Al cannot account for the ≈ 0.7 eV barrier. Instead, the thickness variations of ϕ_s and qV_B in Fig. 1 show that two electronic processes occur—dipole formation saturating at submonolayer coverage and band bending reaching completion at multilayer coverage as the bulk metal forms. The initial state of dipole formation encompasses the two steps of bond saturation and interface region formation proposed by Margaritondo, Rowe, and Christman.⁷

SPS measurements indicate that new states 0.6–0.7 eV below E_c accompany the dipole formation at submonolayer coverage. These features further demonstrate that the extrinsic phenomena of the interface rather than any intrinsic surface states of the semiconductor account for the S-B formation.

The magnitude of charge redistribution at the

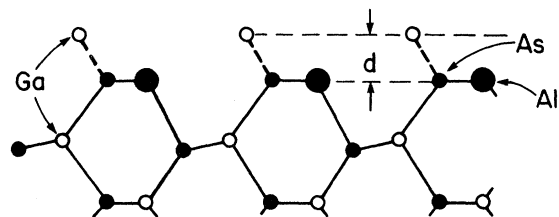


FIG. 3. Cross-sectional view of GaAs(110) surface with Al in Ga lattice site, nearly free Ga above surface, and dipole length d .

M-S interface can be estimated from the measured interfacial dipole and the local atomic rearrangement. Figure 3 illustrates the Al-GaAs(110) interface at the monolayer level with surface Ga atoms replaced by Al and nearly free Ga ordered on the outer surface, consistent with LEED and with the much more stable heat of formation of AlAs ($-27.8 \text{ kcal mol}^{-1}$) versus GaAs ($-17 \text{ kcal mol}^{-1}$). Valence-band spectra suggest that Al induces an unrelaxed GaAs surface structure.¹⁰ These spectra indicate the removal by Al of a state located -4.2 eV below the GaAs valence-band edge, which Chadi has found to be characteristic of the relaxed²¹ versus the unrelaxed surface.²² Recently, Mele and Joannopoulos have accounted for all electronic features reported here with a tight-binding calculation involving surface counterrelaxation and charge redistribution among all three constituents.²³ Thus, the Al bonding and relaxation in Fig. 3 differ from the model of Ref. 13 for metal bonding to one half of the surface atoms in a relaxed configuration. For the unreconstructed surface shown in Fig. 3, the dipole length perpendicular to the surface is 2 \AA . The resultant charge transfer away from the surface is only 0.17 electron/atom and can vary by at most 30%, depending on the surface relaxation and dipole width. For comparison, tight-binding calculations predict a 0.2 electron transfer from As to Ga in bulk GaAs.^{24,25}

The atomic structure and charge redistribution provide a useful comparison with Al-GaAs interface calculations. The dipole extent and direction of charge transfer are consistent with pseudopotential calculations⁴ which indicate metal-induced charge tailing¹⁷ only a few angstroms into the semiconductor with the charge on the outermost semiconductor atoms more negative than in the bulk. The charge transfer reported here is substantially more than the <0.002 electron transfer predicted for the bulk AlAs-GaAs interface.²⁵ This charge transfer and the initial $\Delta\phi_s = 0.45 \text{ eV}$ of the first AlAs interface layer may be a reflection of the 0.4-eV conduction-band discontinuity expected for an AlAs-GaAs heterojunction.^{25,26} Furthermore, the appearance of new interface states confirms theoretical predictions of metal-induced states within the band gap.⁴ In particular, such states have been predicted by Chelikowsky, Louie, and Cohen for a half monolayer of Al bonded solely to As sites with no cation relaxation.⁵

In summary, we have demonstrated that a well-defined chemical reaction at the microscopic

Al-GaAs(110) interface has a dominant effect on the electronic structure and that the microscopic charge redistribution at the junction is responsible for the macroscopic Schottky-barrier height.

The authors thank C. B. Duke, E. J. Mele, and D. J. Chadi for stimulating discussions, and the Stanford Synchrotron Radiation Laboratory staff for their experimental support. This work was partially supported by National Science Foundation Grant No. CMR 73-07692 in cooperation with the Stanford Linear Accelerator Center and the U. S. Energy Research and Development Administration.

¹S. Kurtin, T. C. McGill, and C. A. Mead, *Phys. Rev. Lett.* **22**, 1433 (1970).

²L. J. Brillson, *Phys. Rev. B* **18**, 2431 (1978).

³L. J. Brillson, *J. Vac. Sci. Technol.* **15**, 1378 (1978).

⁴S. G. Louie and M. L. Cohen, *Phys. Rev. Lett.* **35**, 866 (1975), and *Phys. Rev. B* **13**, 2461 (1976); S. G. Louie, J. R. Chelikowsky, and M. L. Cohen, *Phys. Rev. B* **15**, 2154 (1977).

⁵J. R. Chelikowsky, S. G. Louie, and M. L. Cohen, *Solid State Commun.* **20**, 641 (1976).

⁶R. Z. Bachrach, S. A. Flodström, R. S. Bauer, S. B. M. Hagström, and D. J. Chadi, *J. Vac. Sci. Technol.* **15**, 488 (1978); R. Z. Bachrach, *J. Vac. Sci. Technol.* **15**, 1340 (1978).

⁷J. E. Rowe, G. Margaritondo, and S. B. Christman, *Phys. Rev. B* **15**, 2195 (1977); G. Margaritondo, J. E. Rowe, and S. B. Christman, *Phys. Rev. B* **14**, 5396 (1976).

⁸R. Z. Bachrach and A. Bianconi, *J. Vac. Sci. Technol.* **15**, 525 (1978).

⁹L. J. Brillson, in *Proceedings of the Fourteenth International Conference on the Physics of Semiconductors*, edited by R. A. Stradling (Plessey, Edinburgh, 1978).

¹⁰R. Z. Bachrach, R. S. Bauer, J. C. McMennamin, and A. Bianconi, in *Proceedings of the Fourteenth International Conference on the Physics of Semiconductors*, edited by R. A. Stradling (Plessey, Edinburgh, 1978).

¹¹I. Lindau, P. W. Chye, C. M. Garner, P. Pianetta, and W. E. Spicer, *J. Vac. Sci. Technol.* **15**, 1332 (1978).

¹²L. J. Brillson, *Phys. Rev. Lett.* **40**, 260 (1978).

¹³J. E. Rowe, S. B. Christman, and G. Margaritondo, *Phys. Rev. Lett.* **35**, 1471 (1975).

¹⁴G. Leonhardt, A. Berndtsson, J. Hedman, M. Klansen, R. Nilsson, and C. Nordling, *Phys. Status Solidi (b)* **60**, 241 (1973).

¹⁵R. Ludeke and L. Esaki, *Surf. Sci.* **47**, 132 (1975).

¹⁶J. van Laar and A. Huijser, *J. Vac. Sci. Technol.* **13**, 769 (1976).

¹⁷V. Heine, *Phys. Rev.* **138**, A1689 (1963).

¹⁸C. A. Mead, *Solid State Electron.* **9**, 1023 (1966).

¹⁹A. Y. Cho and P. D. Dernier, *J. Appl. Phys.* **49**, 3328 (1978).

- ²⁰P. O. Cortland, Surf. Sci. **62**, 183 (1977).
²¹A. R. Lubinsky, C. B. Duke, R. W. Lee, and P. Mark, Phys. Rev. Lett. **36**, 1058 (1976).
²²D. J. Chadi, Phys. Rev. B (to be published).
²³E. J. Mele and J. D. Joannopoulos, to be published.
²⁴E. J. Mele and J. D. Joannopoulos, Phys. Rev. B **17**, 1816 (1978).
²⁵W. E. Pickett, S. B. Louie, and M. L. Cohen, Phys. Rev. B **17**, 815 (1978).
²⁶L. Esaki, L. L. Chang, W. E. Howard, and V. L. Rideout, in *Proceedings of the Eleventh International Conference on the Physics of Semiconductors, Warsaw, 1972*, edited by The Polish Academy of Sciences (Elsevier, Amsterdam, 1972), p. 431.

High-Frequency ac Susceptibility and ESR of a Spin-Glass

E. D. Dahlberg, M. Hardiman, R. Orbach, and J. Souletie^(a)
Physics Department, University of California, Los Angeles, California 90024
 (Received 7 November 1978)

We report the low-field ac susceptibility from 16 Hz to 2.8 MHz on the dilute spin-glass Ag:Mn in the vicinity of the glass temperature, T_G . Within experimental error T_G is frequency independent. We also report electron-spin-resonance measurements in the same samples at 1.6 and 9.1 GHz. The differences in the ESR data at two frequencies appear to be due to the different fields for resonance and not to the different measuring frequencies.

Several of the theories^{1,2} which consider the zero-field-cooled spin-glass state³ to be metastable predict an increase in T_G , the spin-glass temperature for the ac susceptibility maximum, with increasing ac measuring frequency, ν . All previously reported ac susceptibility measurements on spin-glasses have been made at relatively low frequencies (<5 kHz). However, electron spin resonance data taken at 9 GHz on spin-glass systems⁴ have been characterized by the temperature at which the resonance g value departs from its high-temperature (paramagnetic) value, T_{gv} , or by the temperature where the resonance linewidth passes through a minimum value, T_{min} . Both these temperatures are considerably larger than the low-frequency ac-susceptibility T_G value and have been interpreted⁵ as the effective glass temperature, T_G^* , at 9 GHz. In recent neutron-scattering experiments,⁶ T_G^* was taken as the temperature of the peak in the quasi-elastic-scattering cross section. Again T_G^* was found to be greater than T_G . The effective measurement frequency was here assumed to be the reciprocal of the instrumental resolution time ($\sim 10^{-11}$ s). The large gap in frequency between previous ac measurements and the ESR and neutron measurements ($\sim 10^3$ to $\sim 10^{11}$ Hz) has prompted this work.

We report here new measurements on the low-field ac susceptibility, $\chi'(\nu, T)$, and ESR of dilute Ag:Mn spin-glass alloys in the vicinity of T_G . In particular our ac measurements extend to much higher frequencies (2.8 MHz) than in previous

studies, and our ESR measurements are made at two well-separated frequencies. No evidence is found for any frequency dependence in the behavior of the ac-susceptibility spin-glass peak over five decades in frequency (16 Hz to 2.8 MHz). The quantitative differences seen in the ESR results in 1.6 and 9.1 GHz are shown to be due, at least in part, to the different fields for resonance and not to the different measuring frequencies.

Five master ingots of Ag:Mn with Mn concentrations of 1, 2, 3, 4, and 5×10^3 atomic ppm were made by arc-melting 5N (99.999% purity) Ag and 3N (99.9% purity) Mn. They were then given all the same homogenizing anneal at 800°C for 8 h *in vacuo*. All the measurements reported here were taken on samples made from the original five ingots. The ESR samples were grains produced by filing, having limiting dimensions, d , circa 300 μm . The low-frequency (LF) ac measurements (16 to 160 Hz) were made on the ESR samples. For the medium-frequency (MF) ac data (93 Hz to 109 kHz), such filings were sieved to produce a powder with $d \approx 100 \mu\text{m}$. The high-frequency (HF) ac measurements (0.4 to 2.8 MHz) were made on 18- μm rolled foils. None of these samples were further annealed after the preparation treatment. The LF measurements were made with a commercial SQUID (superconducting quantum interference device) magnetometer, the MF measurements with a simple inductance bridge. The HF data were obtained by placing the sample in an inductor which formed part of the tank circuit of an oscillator. The os-